ISSN 2616-5767 Vol.9, Issue 1: 1-12, DOI: 10.25236/AJETS.2026.090101

A Wavelet-Based Noise Reduction Method for Acoustic Signals Combining WOA-VMD Enhancement and Fuzzy Entropy Thresholding

Menghuan Kuang[1,a], Lifeng Chen[1,b], Zhao Xiao[1,c,*], Muyao Chen[2,d], Yanbo Zhao[3,e]

[1]*School of Mechanical and Electrical Engineering, Hunan University of Science and Technology, Xiangtan, China*
[2]*School of Mechanical and Electrical Engineering, China University of Mining and Technology, Beijing, China*
[3]*School of Automation Science and Engineering, South China University of Technology, Guangzhou, China*
[a]*kmh1033509550@163.com,* [b]*1261983652@qq.com,* [c]*3229076867@qq.com,* [d]*2598495369@qq.com,* [e]*1711665205@qq.com*
[*]*Corresponding author*

Abstract: *Strong noise interference during acoustic signal acquisition and modal aliasing during signal processing complicate feature extraction. This paper proposes a novel acoustic signal denoising method that integrates optimized Variational Mode Decomposition (VMD) with wavelet fuzzy entropy. First, the Whale Optimization Algorithm (WOA) is employed to optimize the VMD's mode component K and penalty factor α, thereby suppressing mode aliasing. Subsequently, the minimum envelope entropy is used as the fitness function to select the optimal Intrinsic Mode Function (IMF) component. Finally, fuzzy entropy values are computed for each IMF to further filter noise components. For IMF components dominated by noise, wavelet transform denoising is applied. These denoised components are then reconstructed with the initially filtered useful signal IMF components to obtain the denoised signal. Through noise reduction analysis of acoustic signals collected via a self-built test bench, this method was validated as superior to fixed-parameter VMD decomposition and wavelet threshold denoising algorithms. It effectively removes noise, providing new insights for planetary gear acoustic signal denoising.*

Keywords: *acoustic signal, WOA-VMD, fuzzy entropy, planetary gear, wavelet threshold denoising*

1. Introduction

Currently, planetary gear fault diagnosis typically involves collecting vibration signals for analysis. However, in harsh operating environments where contact measurements are impractical, acoustic signals can capture critical operational information under any conditions. Yet acoustic signals exhibit characteristics such as severe modulation and low signal-to-noise ratio, making them susceptible to environmental noise interference during propagation [1-3]. Therefore, effective noise reduction to enhance acoustic signal quality and SNR is crucial for extracting and identifying fault characteristics in planetary gears.

Existing noise reduction methods for planetary gear fault diagnosis signals primarily include wavelet transform [4], empirical mode decomposition (EMD) and its variants [5], and variational mode decomposition [6] (VMD). Among these, wavelet transform suffers from high computational complexity and requires manual selection of suitable wavelet basis functions. EMD offers strong adaptability but inherently suffers from mode aliasing and end-point effects [7-8]. VMD, as a novel non-linear and non-stationary signal decomposition method, effectively overcomes EMD's modal aliasing problem by constructing a variational constraint model. However, its decomposition effectiveness depends on two parameters: the number of modes K and the penalty factor α. An excessively small K value leads to under-decomposition, while an excessively large K value causes over-decomposition. The selection of the penalty factor α directly affects the modal bandwidth and noise suppression effect [9]. Currently, VMD parameter settings largely rely on manual experience, lacking adaptive optimization mechanisms tailored

ISSN 2616-5767 Vol.9, Issue 1: 1-12, DOI: 10.25236/AJETS.2026.090101

to specific signal characteristics. This limitation restricts its practical application in processing planetary gear acoustic signals under complex operating conditions.

In recent years, numerous scholars have employed intelligent optimization algorithms to optimize VMD's mode count K and penalty factor α. Zhang et al. [10] employed a whale optimization algorithm to optimize VMD for underwater acoustic signals, experimentally demonstrating its ability to effectively enhance signal-to-noise ratio. He et al. [11] adapted a particle swarm optimization algorithm for adaptive parameter tuning of VMD, utilizing correlation coefficients to screen IMF components and applying wavelet threshold denoising to noisy modes. Experimental results confirmed this method's effective noise reduction. Tang Jun et al. [12] employed a triangular topology optimization algorithm for VMD optimization. They screened IMF components for noise using normalized K-nearest neighbor mutual information and applied wavelet threshold denoising. Experimental results confirmed this method's effectiveness in removing noise from hydroacoustic signals. However, existing methods employing correlation coefficients and normalized K-nearest neighbor mutual information as screening metrics exhibit insufficient discrimination between weak useful signals and noise components. In scenarios with strong noise interference, they are prone to erroneously filtering useful signal components or overlooking noise-dominated components, thereby reducing denoising reliability.

In the VMD component selection phase, traditional correlation coefficient methods and energy criteria struggle to effectively distinguish noise-dominated components from fault-feature components. In contrast, calculating complexity metrics for each IMF component based on fuzzy entropy and establishing adaptive thresholds enables effective differentiation between noise and useful feature components. Furthermore, existing denoising methods predominantly employ uniform processing strategies, applying identical denoising intensity to all IMF components without accounting for the distinct noise distribution characteristics across different modes. In contrast, the selective wavelet threshold denoising strategy adopts a sub band filtering approach, applying targeted thresholding to noise-dominated high-frequency IMF components while preserving low-frequency components containing fault features [13]. Zhang Liyao et al. [14] optimized VMD for rotor-bearing systems, selecting IMF components with higher correlation values based on cumulative kurtosis proportions for reconstruction to achieve noise removal. Zhu Yuyao et al. [15] addressed noise in bridge monitoring data by combining an optimized VMD with correlation coefficient thresholds to suppress multiple noise sources. Guo Qinghui et al. [16] denoised noisy modes by improving the wavelet threshold method, reconstructing effective modes from denoised modes, demonstrating significant improvement in signal-to-noise ratio. Liu Kui et al. [17] applied wavelet thresholds to all supercouple signals, which may result in insufficient or excessive noise reduction, failing to adequately preserve the original signal.

Addressing the low SNR and strong nonlinearity of planetary gear sound signals, this paper proposes a wavelet adaptive denoising method based on WOA optimization of VMD parameters and fuzzy entropy thresholds. This method employs the WOA algorithm for global optimization of VMD parameters; introduces fuzzy entropy as an evaluation metric for IMF components to establish an adaptive screening mechanism for precise separation of noise and feature components; and adopts a selective wavelet threshold strategy for differentiated processing of different modal components. This approach effectively enhances the extraction capability of weak planetary gear fault features under strong noise conditions, providing a new technical pathway for early fault diagnosis.

2. Basic Principles

2.1 VMD Decomposition

VMD is an adaptive, fully non-recursive modal variational and signal processing method. This algorithm divides the variational problem into construction and solution phases. By decomposing the input signal f(t) into K IMF components, the constraint that the sum of all modes equals the input signal is imposed. The variational model for the construction process is then formulated as follows:

$$\min_{\{u_k,\omega_k\}}\left\{\sum_k\left\|\partial_t\left[\left(\delta(t)+\frac{j}{\pi t}\right)*u_k(t)\right]e^{-j\omega_k t}\right\|_2^2\right\} \tag{1}$$

$$s.t.\sum_k u_k = f(t) \tag{2}$$

Where $u_k=\{u_1,u_2,\cdots,u_k\}$ denotes the respective modal function, $\omega_k=\{\omega_1,\omega_2\cdots,\omega_k\}$ represents

ISSN 2616-5767 Vol.9, Issue 1: 1-12, DOI: 10.25236/AJETS.2026.090101

the respective modal center frequency, ∂_t is the partial derivative with respect to time t, δ_t is the Dirac delta function, and * denotes convolution.

To address the aforementioned constrained optimization problem, a quadratic penalty term α and the Lagrange multiplier method λ are introduced. This transforms the constrained variational problem into an unconstrained variational problem, yielding the following solution formula:

$$L(\{u_k\},\{\omega_k\},\lambda)=\alpha\sum_k\left\|\partial_t\left[\left(\delta(t)+\frac{j}{\pi t}\right)*u_k(t)\right]e^{-j\omega_k t}\right\|_2^2+\left\|f(t)-\sum_k u_k(t)\right\|_2^2+\left(\lambda(t),\, f(t)-\sum_k u_k(t)\right) \tag{3}$$

Update $u_k^{n+1},\omega_k^{n+1},\lambda_k^{n+1}$ for all $\omega\geq 0$ until the optimal condition is reached, then terminate the iteration and exit the loop. Finally, output the k IMF components.

2.2 Whale Optimization Algorithm

WOA simulates the hunting behavior of humpback whales by modeling their bubble net attack mechanism through a spiral pattern. It employs an optimal search agent to simulate the hunting process, where each whale's position represents a potential solution. By continuously updating whale positions to seek optimal targets, the algorithm ultimately arrives at the optimal solution. The whale encirclement mechanism consists of three primary phases: encircling prey, bubble net feeding, and prey search.

2.2.1 Encircling the Prey

In the WOA algorithm, the whale's search range covers the entire global solution space. Since the optimal design position cannot be known in advance, the current best candidate solution is assumed to be the target prey or a solution close to the optimum. After defining the best search agent, other search agents update their positions toward it. This behavior can be described by the following equation:

$$\vec{D}=\left|\vec{C}\bullet\vec{X}^*(t)-\vec{X}(t)\right| \tag{4}$$

$$\vec{X}(t+1)=\vec{X}^*(t)-\vec{A}\bullet\vec{D} \tag{5}$$

In the formula: $\vec{X}^*(t)$ denotes the currently obtained optimal position vector; $\vec{X}(t)$ denotes the position vector; A and C denote coefficient vectors; t denotes the iteration count; $\|$ denotes absolute value; $\bullet$ denotes multiplication. If a better solution exists, $X^*(t)$ will be continuously updated during each iteration, where $\vec{A}$ and $\vec{C}$ are calculated using the following formula:

$$\vec{A}=2\vec{a}*\vec{r}_1-\vec{a} \tag{6}$$

$$\vec{C}=2*r_2 \tag{7}$$

In the equation, $\vec{a}$ represents the transition from 2 to 0 during the linear iteration process; r_1 and r_2 denote random vectors in the interval [0,1].

2.2.2 Bubble Net Feeding

Humpback whales employ two feeding mechanisms: bubble net feeding and encircling feeding. When utilizing bubble net feeding, the spatial relationship between prey and humpback whales can be described by the following logarithmic spiral equation:

$$\vec{X}(t+1)=\vec{D}'*e^{bl}*\cos(2\pi l)+\vec{X}^*(t) \tag{8}$$

$$\vec{D}'=\left|\vec{X}^*(t)-X(t)\right| \tag{9}$$

In the formula: D' denotes the distance between the current search individual and the current optimal solution; B epresents the spiral shape parameter; l denotes a random number uniformly distributed in the range [-1,1]; b is a constant.

When approaching prey, WOA selects between bubble net predation or retraction-based encirclement based on the predation mechanism probability P. The spatial relationship is described by the following

ISSN 2616-5767 Vol.9, Issue 1: 1-12, DOI: 10.25236/AJETS.2026.090101

formula:

$$X=(t+1)\begin{cases}\vec{X}^{*}(t+1)-\vec{A}*\vec{D} & 0\le p\le 0.5\\ \vec{D}'*e^{bl}*\cos(2\pi l)+\vec{X}^{*}(t) & 0.5<p\le 1\end{cases} \tag{10}$$

As the iteration count t increases, the parameter A and convergence factor a gradually decrease. If |A|<1, the whales gradually encircle the current optimal solution.

2.2.3 Searching for Prey

To ensure all whales fully explore the solution space, WOA updates positions based on mutual distances between whales, thereby achieving random search. Thus, when |A| ≥1, the search agent moves toward a randomly selected whale.

$$\vec{D}''=\left|\vec{C}\bullet\vec{X}_{rand}(t)-\vec{X}(t)\right| \tag{11}$$

$$\vec{X}(t+1)=\vec{X}_{rand}(t)-\vec{A}\bullet\vec{D} \tag{12}$$

In the formula: D'' denotes the distance between the current search individual and the random individual; $X_{rand}(t)$ denotes the position of the current random individual.

2.3 Minimum Envelope Entropy and Fuzzy Entropy

2.3.1 Minimum Envelope Entropy

By setting the minimum envelope entropy as the fitness function, envelope entropy characterizes the sparsity of the original signal: if an IMF contains high noise levels and lacks effective feature information, its envelope entropy value will be large; conversely, the envelope entropy value will be relatively smaller. Minimum envelope entropy can be calculated using the following formula:

$$\begin{cases}E_p=-\sum_{j=1}^{N}p_j\lg p_j\\ p_j=a(j)\Big/\sum_{j=1}^{N}a(j)\end{cases} \tag{13}$$

In the equation: $a(j)$ denotes the envelope signal obtained by Hilbert demodulation of the k modal components resulting from VMD decomposition; $p(j)$ denotes the probability distribution sequence; N denotes the number of sampling points; the entropy value of $p(j)$ is the minimum envelope entropy E_p.

2.3.2 Fuzzy Entropy

Fuzzy entropy is an improved algorithm based on approximate entropy and sample entropy, measuring the probability of generating new patterns in a time series when its dimensionality changes. The higher the probability, the greater the sequence's complexity and the larger its entropy value. Fuzzy entropy is defined as follows:

For a given time series $\{x(i),i=1,2,3,\cdots,N\}$, the similarity of fuzzy entropy is:

$$D_{ij}^{m}=\mu\left(d_{ij}^{m},n,r\right)=e^{-\ln 2\left(d_{ij}^{m}/r\right)^{m}} \tag{14}$$

The vaguely defined evaluation function is:

$$\varphi^{m}(n,r)=\frac{1}{N-m}\sum_{i-1}^{N-m}\left(\frac{1}{N-m-1}\sum_{j=1,j\neq 1}^{N-m}D_{ij}^{m}\right) \tag{15}$$

Using the evaluation function, define the fuzzy entropy FE as:

ISSN 2616-5767 Vol.9, Issue 1: 1-12, DOI: 10.25236/AJETS.2026.090101

$$\varphi^m(n,r)=\frac{1}{N-m}\sum_{i-1}^{N-m}\left(\frac{1}{N-m-1}\sum_{j=1,j\neq 1}^{N-m}D_{ij}^m\right) \tag{16}$$

In the formula: r denotes the similarity tolerance; n represents the boundary gradient of the fuzzy function; d_{ij}^m indicates the distance between X_i^m and X_j^m; m denotes the pattern dimension.

2.4. Selective Wavelet Threshold Denoising

Wavelet threshold denoising effectively removes noise while preserving useful signal components by decomposing the signal into different frequency components via wavelet transform, followed by threshold processing and reconstruction of these components. Traditional wavelet threshold denoising methods apply a uniform threshold directly to the signal. While computationally straightforward, this approach has limitations when applied to non-stationary, nonlinear planetary gear fault acoustic signals. To address this, this paper improves upon the traditional wavelet threshold denoising strategy by adopting a hierarchical processing architecture:

(1) Decompose the original signal ft into K IMF components using optimized VMD parameters:

$$f(t)=\sum_{k=1}^{k}u_k(t) \tag{17}$$

(2) Based on fuzzy entropy thresholds, the IMF components are divided into two sets:

$$\begin{cases}U_{useful}=\{u_k(t)|FE_k\le T_{FE}\}\\ U_{noise}=\{u_k(t)|FE_k>T_{FE}\}\end{cases} \tag{18}$$

(3) Apply wavelet thresholding only to noise-dominated components:

$$\hat{u}_k(t)=\begin{cases}u_k(t) & u_k(t)\in U_{useful}\\ WTDenoise(u_k(t)) & u_k(t)\in U_{noise}\end{cases} \tag{19}$$

In the formula: $WTDenoise(\bullet)$ denotes the wavelet threshold operation.

(4) Reconstruct the processed components into a denoised signal:

$$\hat{f}(t)=\sum_{u_k\in U_{useful}}u_k(t)+\sum_{u_k\in U_{noise}}\hat{u}_k(t) \tag{20}$$

3. Fuzzy Entropy Wavelet Threshold Noise Reduction Based on WOA-VMD Parameter Optimization

This paper proposes a novel method for planetary gear noise reduction in acoustic signals by optimizing the combination of Variational Modal Decomposition (VMD) and fuzzy entropy wavelet threshold using a whale optimization algorithm. To select the optimal number of modes K and penalty factor α, the minimum envelope entropy value is employed as the fitness function. After VMD decomposition, a smaller envelope entropy value indicates less noise contained within the IMF components.

As shown in Figure 1, the noise reduction algorithm described in this paper is as follows:

(1) In the process of optimizing VMD parameters using WOA, initialization of algorithm optimization parameters is performed first, simultaneously initializing the population positions in the whale optimization algorithm. Each individual within the population corresponds to a set of variational mode decomposition parameters: Number of modes K, penalty factor α. Subsequently, each individual performs VMD decomposition on the original signal using its (K, α) parameters. The fitness function is defined as the minimum envelope entropy of each intrinsic mode function (IMF). The fitness value for each individual is calculated, and the position of the optimal individual in the current population is recorded. After executing the WOA optimization strategy, when the iteration limit is reached, the optimal VMD parameter combination (K, α) obtained from the current optimization is output.

(2) Based on the optimal VMD parameters (K, α) obtained above, perform VMD decomposition on

ISSN 2616-5767 Vol.9, Issue 1: 1-12, DOI: 10.25236/AJETS.2026.090101

the original input signal, decomposing it into several IMF components.

(3) For each IMF component obtained after VMD decomposition, calculate its corresponding fuzzy entropy value. Based on a preset fuzzy entropy threshold, classify each IMF component as either noise-dominant or useful signal.

(4) Apply wavelet threshold denoising to suppress noise in IMF components classified as noise-dominant.

(5) The useful signal components are fused and reconstructed with the noise-dominant components after wavelet threshold denoising, ultimately yielding the target signal with completed noise reduction.

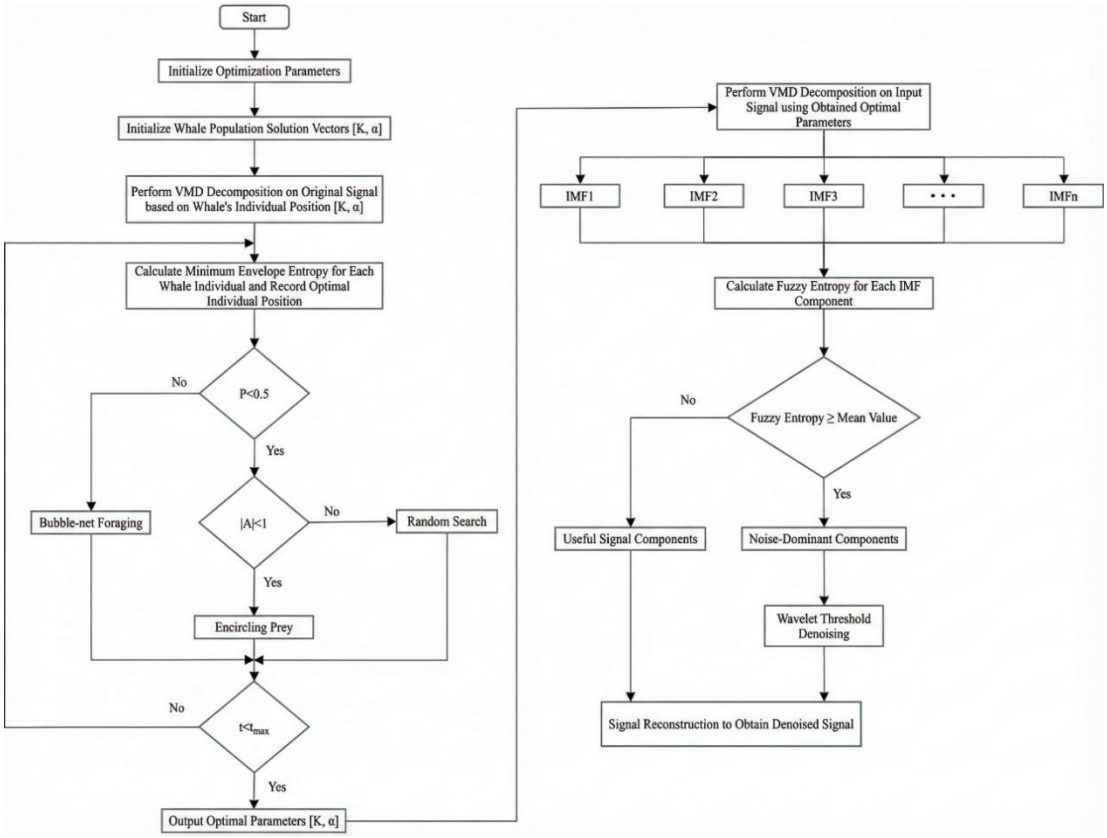

Figure 1. Noise Reduction Algorithm Flowchart.

4. Experimental Verification and Analysis

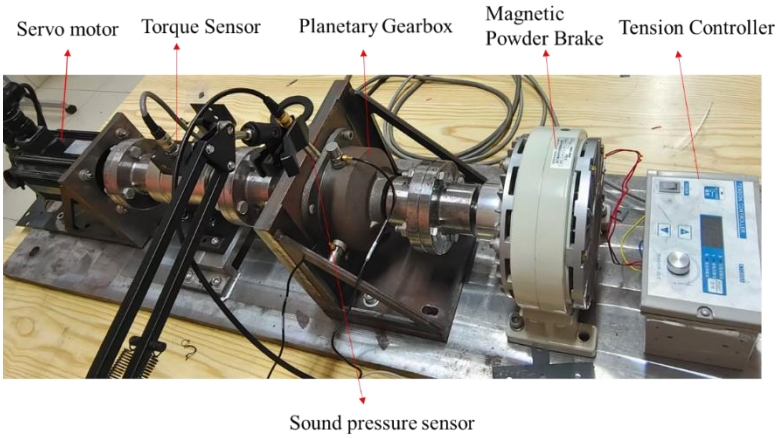

Figure 2. Planetary Gear Transmission Simulation Experiment Platform.

This paper employs a constructed planetary gear transmission simulation test platform for fault signal

ISSN 2616-5767 Vol.9, Issue 1: 1-12, DOI: 10.25236/AJETS.2026.090101

acquisition. The physical diagram of the simulation test bench is shown in Figure 2. The test bench comprises a servo motor, torque sensor, planetary gearbox, magnetic powder brake, tension controller, and sound pressure sensor. The sound pressure sensor model is AWA14423, featuring a nominal sensitivity of 50 mV/Pa and a frequency response range of 10–20 kHz.

To validate the noise reduction effectiveness of the proposed algorithm, the sun gear in a planetary gearbox under both normal and tooth-fractured conditions was selected as the research subject. First, parameter optimization was performed using WOA-VMD to obtain the optimal model for decomposition parameters. The parameter settings for the whale optimization algorithm are shown in Table 1. Using minimum envelope entropy as the fitness function, the optimal result combination for the normal signal was K=6, α=375, with a minimum envelope entropy value of 6.8834. The optimal result for the tooth-fracture signal was K=13, α=1.588, yielding a minimum envelope entropy value of 7.2119. The iteration curves are shown in Figures 3 and 4.

Table 1: Whale Optimization Algorithm Parameter Settings.

Parameters	Numerical Values
Population Size	8
Maximum Iteration Count	25
Number of Modes Range	[2~14]
Penalty Factor Range	[100~11000]
Number of Variables	2

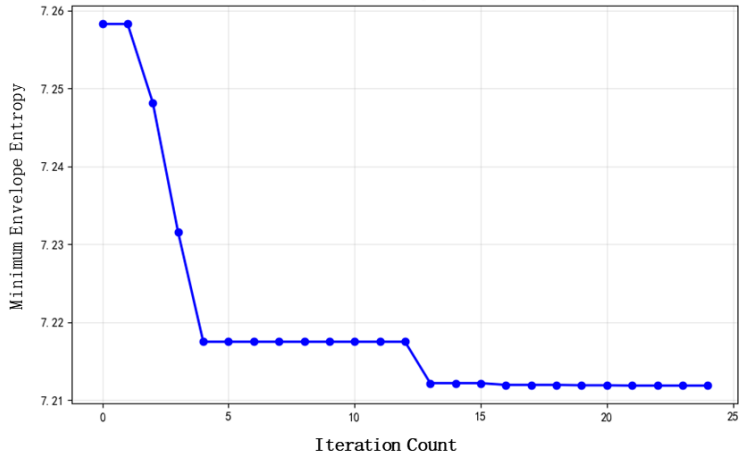

Figure 3: Iterative Convergence Curve of Normal Signal.

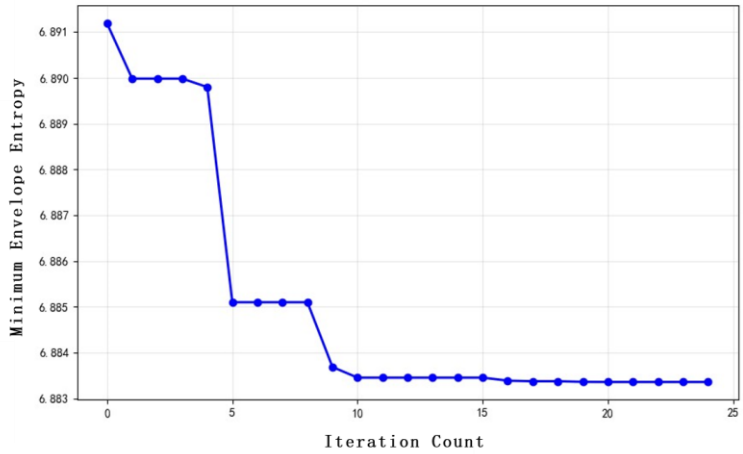

Figure 4: Iterative Convergence Curve of Tooth Breakage Signal.

The optimal number of parameters K obtained via WOA-VMD is used to calculate the fuzzy entropy values for each IMF component. The fuzzy entropy values of IMF components under different conditions are shown in Table 2. The mean fuzzy entropy serves as the criterion for distinguishing useful components from noise components. The mean fuzzy entropies for normal signals and tooth-gap signals

ISSN 2616-5767 Vol.9, Issue 1: 1-12, DOI: 10.25236/AJETS.2026.090101

are 0.0348 and 0.0072, respectively. Therefore, IMF1 to IMF3 in the normal signal and IMF1 to IMF4 in the tooth gap signal are noise components, while the remaining components are useful. Wavelet threshold denoising is applied to the components identified as noise, and the denoised signal is reconstructed with the useful signal.

Table 2: Fuzzy Entropy Values of IMF Components under Different Conditions.

Type	Fuzzy Entropy Component Threshold for Normal Signals	Fuzzy Entropy Component Threshold for Tooth-Drop Signals
IMF1	0.0540	0.0195
IMF2	0.0636	0.0259
IMF3	0.0596	0.0178
IMF4	0.0214	0.0119
IMF5	0.0066	0.0056
IMF6	0.0038	0.0041
IMF7		0.0026
IMF8		0.0031
IMF9		0.0022
IMF10		0.0007
IMF11		0.0001
IMF12		0.0001
IMF13		0.0001

To validate the reliability of the proposed denoising method, comparisons were conducted with the wavelet threshold and fixed VMD parameter approaches. Their time-domain plots are shown in Figures 5 through 10. Blue indicates the original signal, while red represents the denoised signal. Observation reveals that under normal signals, the wavelet threshold method excessively smooths some useful signals while failing to completely eliminate noise; while the fixed-parameter VMD method suppresses noise but retains some high-frequency noise components. The proposed method achieves the most pronounced noise reduction, exhibiting high signal smoothness while preserving key signal features. For tooth-break signals, both the wavelet threshold and fixed-parameter VMD methods produce overall smooth signals but suffer severe loss of critical fault feature information. In contrast, the proposed method yields more regular signal morphology with clearly discernible fault features, while significantly reducing background noise.

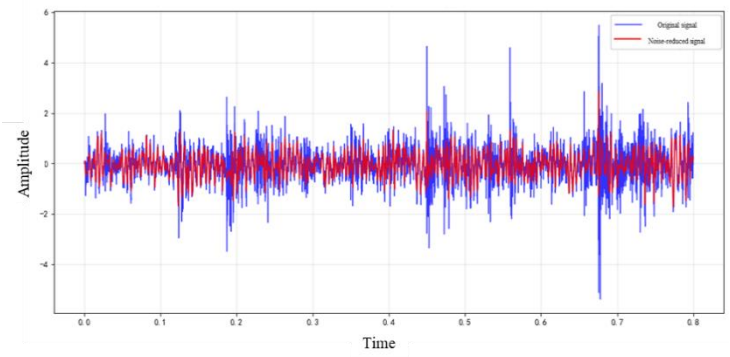

Figure 5: Time-domain plots before and after wavelet threshold denoising under normal signal conditions.

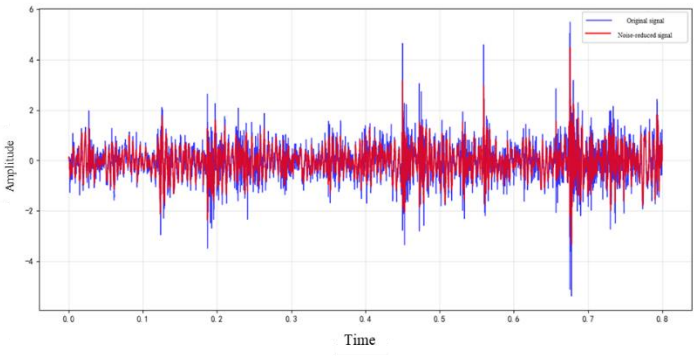

Figure 6: Time-domain plots before and after noise reduction with fixed VMD parameters under normal signal conditions.

ISSN 2616-5767 Vol.9, Issue 1: 1-12, DOI: 10.25236/AJETS.2026.090101

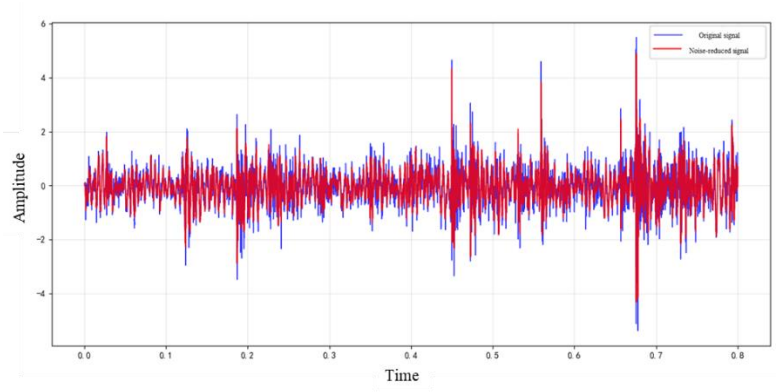

Figure 7: Time-domain plots of normal signals before and after noise reduction using the proposed method.

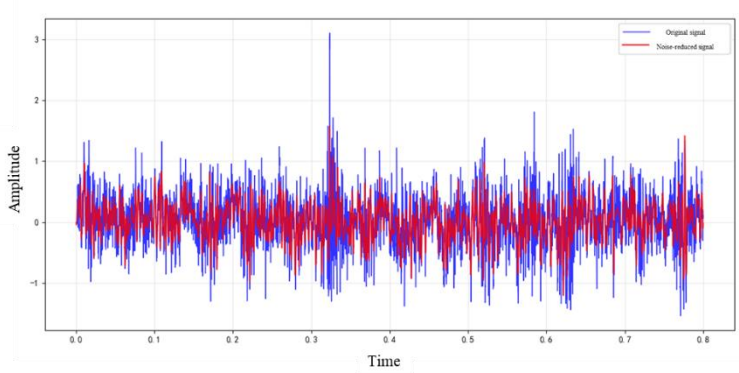

Figure 8: Time-domain plots before and after wavelet threshold denoising under tooth-gap signals.

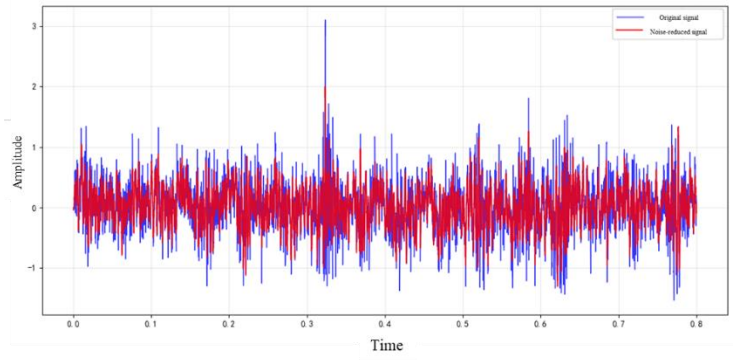

Figure 9: Time-domain plots before and after noise reduction with fixed VMD parameters under tooth dropout signals.

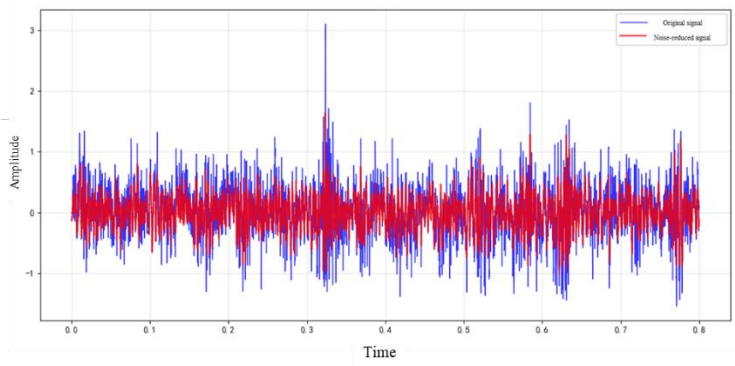

Figure 10: Time-domain plots before and after noise reduction using the proposed method under tooth-dropout signals.

ISSN 2616-5767 Vol.9, Issue 1: 1-12, DOI: 10.25236/AJETS.2026.090101

To demonstrate the superiority of noise reduction performance, the signal-to-noise ratio (SNR) and root mean square error (RMSE) are employed to evaluate the noise reduction effectiveness of the three methods. Generally, a higher SNR and lower RMSE indicate better noise reduction results. The evaluation metrics for different noise reduction methods are shown in Table 3.

As shown in Table 3, the proposed method achieves a higher signal-to-noise ratio than both the wavelet threshold and fixed VMD parameter methods under both normal and tooth-break conditions. Additionally, its root mean square error is lower than the other two methods. This indicates that the proposed method delivers the best noise reduction performance, with the reconstructed acoustic signal after noise reduction most closely approximating the true acoustic signal.

Table 3 Evaluation Metrics for Different Noise Reduction Methods

Noise Reduction Method	State	Signal-to-Noise Ratio	Root Mean Square Error
Fixed VMD Parameters	Normal	6.27	0.3083
	Tooth Breakage	5.30	0.2271
Wavelet Threshold	Normal	3.58	0.4200
	Tooth Breakage	3.52	0.2790
Proposed Method	Normal	7.03	0.2825
	Tooth Breakage	5.51	0.2068

After noise reduction using the method described in this paper, under normal operating conditions, the meshing frequency f_m (approximately 230.77 Hz) exhibits sidebands appearing at frequencies $f_m + nf_c\,(n=1,2,\cdots)$ with sideband intervals corresponding to the planetary carrier rotation frequency f_c (approximately 3.85 Hz). Some dominant sideband peak frequencies differ by $3f_c$, such as f_m+6f_c、f_m-2f_c and f_m-6f_c in Figure 11; The characteristic frequency of a local sun gear fault is $f_s=(3f_m)/Z_s=N(f_s^{(r)}-f_c)$, Sideband peaks will appear at frequencies $f_m \pm kf_c+(n\pm k/N)f_s$, such as the $f_m+2/3\,f_s$, $f_m+5f_c-f_s$ and f_m+3f_c in Figure 12, which aligns with the fault characteristic frequency. The denoised spectrum clearly indicates a sun gear fault, consistent with actual conditions, demonstrating the effectiveness of the proposed denoising method.

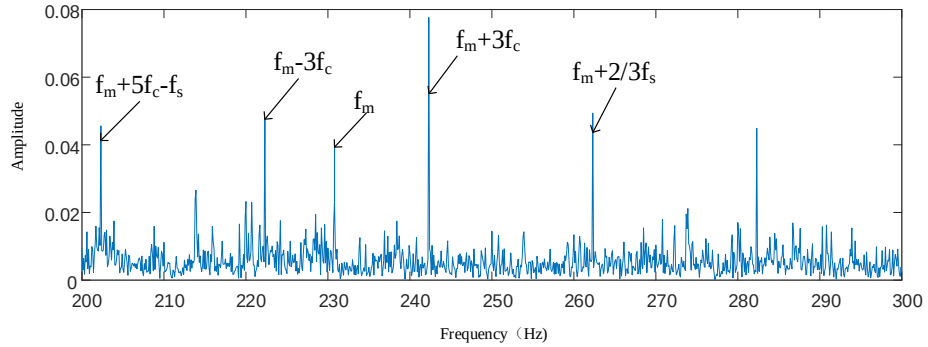

Figure 11: Normal Signal Spectrum.

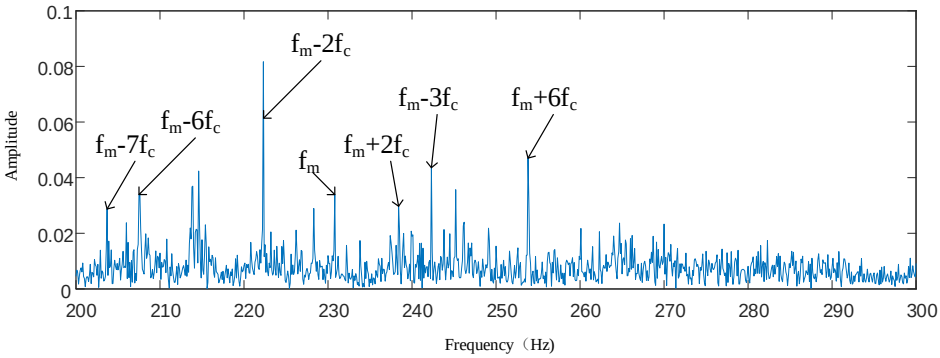

Figure 12: Broken Tooth Signal Spectrum.

ISSN 2616-5767 Vol.9, Issue 1: 1-12, DOI: 10.25236/AJETS.2026.090101

5. Conclusion

This paper addresses issues such as low signal-to-noise ratio in planetary gearbox acoustic signals, severe interference from environmental noise, and modal aliasing during signal decomposition. This paper innovatively proposes an adaptive noise reduction method that integrates the Whale Optimization Algorithm (WOA) to optimize Variational Modal Decomposition (VMD) parameters, fuzzy entropy for intelligent component selection, and selective wavelet thresholding for noise reduction. The method first employs the WOA algorithm with minimum envelope entropy as the fitness function to adaptively optimize the VMD parameter combination (K, α), achieving optimal signal decomposition. Second, it calculates the fuzzy entropy of each IMF component and uses its mean as a threshold to distinguish noise-dominated components from fault-featured useful components; finally, only the noise-dominated IMF undergoes wavelet threshold processing and is reconstructed with the retained useful components. Experimental analysis of acoustic signals from planetary gears under normal and tooth-fracture conditions demonstrates that compared to fixed-parameter VMD and traditional wavelet thresholding methods, the proposed approach achieves superior performance in both signal-to-noise ratio and root mean square error metrics. This provides a reliable new approach for early fault diagnosis of planetary gears based on acoustic signals.

Acknowledgements

The paper was funded by the Hunan Provincial Natural Science Foundation of China (Grants Nos. 2024JJ8275 and 2024JJ2031).

References

[1] Wan A ,Zhu Z ,Bukhaiti A K , et al.Fault diagnosis of helicopter accessory gearbox under multiple operating conditions based on feature mode decomposition and multi-scale convolutional neural networks[J].Applied Soft Computing,2025,113403-113403.

[2] Zhang J ,Zhang S ,Dong Y , et al.Enhanced gear fault diagnosis via heterodyne downconversion: Theoretical verification and optimized ultrasonic signal acquisition[J]. Measurement, 2025, 256(PB):118215-118215.

[3] Wang Lijin. Research on Fault Diagnosis of Transmission Gearboxes Based on Acoustic Signals [D]. Shijiazhuang University of Railways, 2022. DOI: 10.27334/d.cnki.gstdy.2022.000711.

[4] Wu H ,Zhi S ,Fang Q , et al.Adaptive matching squeezing chirplet transform for fault diagnosis of wind turbine planetary gearbox under non-stationary conditions.[J].ISA transactions,2025,

[5] Meng G ,An Y ,Zhang D , et al.Fault diagnosis of gearboxin wind turbine based on EMD-DCGAN[J].EAI Endorsed Transactions on Energy Web,2024,11(1).

[6] Cao J ,Zhang X ,Wang H , et al.A novel approach of fault diagnosis for gearbox based on VMD optimized by SSA and improved RCMDE[J].Journal of Vibration and Control,2025,31(15-16):3282-3294.DOI:10.1177/10775463241272983.

[7] Sun Kang, Jin Jiangtao, Li Chun, et al. Fault Diagnosis of Wind Turbine Gearboxes Based on Improved Empirical Wavelet Transform and Fractal Feature Set [J]. Journal of Solar Energy, 2023, 44(05): 310-319.

[8] Xie Fengyun, Wang Gan, Shang Jiandong, et al. Gearbox Fault Diagnosis Based on Adaptive Variational Modal Decomposition [J]. Propulsion Technology, 2024, 45(09): 223-232.

[9] Guo Qinghui, Li Yuan, Xing Zuoxia. Signal Denoising Method Based on Optimized Variational Modal Decomposition Combined with Wavelet Thresholding [J]. Systems Science and Mathematics, 2025, 45(06): 1687-1700.

[10] Zhang Weiping, Fu Min, Zhang Haiyan, et al. Application of an Improved WOA-VMD Algorithm in Underwater Acoustic Signal Denoising [J]. Journal of Ocean University of China (Natural Science Edition), 2023, 53(01): 138-146.

[11] He Chengbing, Che Qixiang, Xu Zhenhua, et al. Signal Denoising Method Based on Parameter Self-Optimizing Variational Modal Decomposition [J]. Vibration and Shock, 2023, 42(19): 283-293.

[12] Tang Jun, Lei Wensheng, Lin Ling, et al. An Optimized VMD-IWTD Algorithm for Underwater Robot Acoustic Signal Denoising [J/OL]. Machinery Science and Technology, 1-9 [2025-12-01].

[13] Zheng Yang, Zhang Yi, Deng Ruiji, et al. Bridge Monitoring Signal Denoising Method Combining CPO-VMD with Improved Wavelet Threshold [J/OL]. Vibration and Shock, 1-11 [2025-12-02].

[14] Zhang Liyao, Lu Kaiting, Jiang Haiyan, et al. Research on WOA-VMD-Based Signal Decomposition and Reconstruction Method for Rotor-Bearing Systems [J]. Thermal Power Engineering, 2025, 40(02):

ISSN 2616-5767 Vol.9, Issue 1: 1-12, DOI: 10.25236/AJETS.2026.090101

158-166.
[15] Zhu Yuyao, Li Shuangjiang, Xin Jingzhou, et al. Noise Reduction Method for Bridge Monitoring Data Based on GWO-VMD and Correlation Coefficient Threshold [J]. Noise and Vibration Control, 2025, 45(04): 116-122+196.
[16] Guo Qinghui, Li Yuan, Xing Zuoxia. Signal Denoising Method Based on Optimized Variational Modal Decomposition Combined with Wavelet Thresholding [J]. Systems Science and Mathematics, 2025, 45(06): 1687-1700.
[17] Liu Kui, Zhang Dongmei, Yu Guang, et al. Experimental Study on Wavelet Threshold Filtering for Air-Coupled Ultrasonic Signals [J]. Transactions of the Chinese Society for Mechanical Engineering, 2015, 51(20): 61-66.